JOURNAL OF BIOMOLECULAR STRUCTURE AND DYNAMICS
https://doi.org/10.1080/07391102.2020.1794970

Taylor & Francis
Taylor & Francis Group

EXPRESS COMMUNICATION

Natural derivatives with dual binding potential against SARS-CoV-2 main protease and human ACE2 possess low oral bioavailability: a brief computational analysis

Priyanka Sharma and Asifkhan Shanavas

Inorganic & Organic Nanomedicine Lab, Institute of Nano Science and Technology, Mohali, Punjab, India

Communicated by Ramaswamy H. Sarma

ABSTRACT

The world is witnessing severe health meltdown due to COVID-19. Generic antiviral drug remdesivir has been found to reduce time to clinical recovery but with insignificant clinical benefits and the antimalarial drug, hydroxychloroquine has been red flagged by USFDA for use as a prophylactic measure due to its cardiotoxicity. There is an acute requirement for a drug candidate that has significant clinical benefit with minimal to no side effects. With restricted access to wet laboratory techniques, an alternative approach is to engage in computational screening of lead molecules that could inhibit SARS-CoV-2 at different stages of its infectious cycle. Several *in silico* studies on natural derivatives, especially that present in daily refreshments (tea and fruit juices), staple food (black rice, red onions, soy beans etc) and traditional medicines (extracts of herbs, leaves and flowers) have been identified as potential drug candidates that bind efficiently with the key viral proteins. However, oral bioavailability of these nutriments is considerably low due to either poor permeability or loss of structure and function due to digestion in the gastrointestinal tract. Here we discuss few natural secondary metabolites (Delphinidin 3,5-diglucoside, Scutellarein 7-glucoside, Avicularin and 3,5-Di-O-galloylshikimic acid) that showed encouraging binding affinity against coronavirus main protease (M^{pro}) and human ACE2 receptor with MM-GBSA energies up to −74.0 Kcal/mol and −79.5 Kcal/mol, respectively. However, their Abbott bioavailability score (ABS) of 0.11 or 0.17 predicts poor oral bioavailability. This study could trigger interest to engineer potential natural products in managing present or future pandemics.

Abbreviations: Abbot bioavailability score: (ABS), predicts the probability of a compound to have > 10% oral bioavailability in a rat model; ADME is an abbreviation in pharmacokinetics and pharmacology for 'absorption, distribution, metabolism, and excretion', used to describes the disposition of a pharmaceutical compound within an organism; ADME: is an abbreviation in pharmacokinetics and pharmacology for 'absorption, distribution, metabolism, and excretion', used to describes the disposition of a pharmaceutical compound within an organism; COVID-19: Coronavirus disease 2019; main protease (M^{pro}): a cysteine protease, the main target for antiviral drugs against SARS and other coronavirus infections; Angiotensin-Converting Enzyme 2 (ACE2: a type I transmembrane metallocarboxypeptidase utilized by SARS-CoV-2 as a cellular entry receptor; MM-GBSA: molecular mechanics energies combined with generalized born and surface area, to enhance the binding affinity predictions; MM-GBSA: molecular mechanics energies combined with generalized born and surface area, to enhance the binding affinity predictions; severe acute respiratory syndrome corona virus-2 (SARS-CoV-2): virus that cause COVID-19 disease; Swiss ADME: a tool to predict ADME parameters, pharmacokinetic properties, drug like nature.

ARTICLE HISTORY
Received 13 June 2020
Accepted 1 July 2020

KEYWORDS
Natural products; COVID; SARS-CoV-2; ACE2; bioavailability

Introduction

Novel SARS-CoV2 is a pathogenic strain of coronavirus that is raising major concerns over the public health around the world. Coronaviruses are spherical enveloped viruses with positive sense single stranded RNA genome having a place in the Coronaviridae family and they cause respiratory tract infections in humans, animals and birds. SARS-like CoVs isolated from bats have 95% genome sequence identity with human SARS-CoVs, allowing them to directly infect humans without any requirement for an intermediate host (Hu et al., 2018). The genome of SARS coronaviruses comprise 5′ open reading frame ORF (1a and 1b coding region, S region encodes spike glycoprotein, E region encodes enveloped protein, M region encodes membrane protein, N region encodes nucleocapsid protein, six accessory proteins encoded by ORF 3a, ORF 6, ORF 7a, ORF 7b, ORF 8 and 3′ terminal non-coding region) (Rota et al., 2003). The trimeric S glycoprotein contains two S1 and S2 subunits for interaction with host cell receptor and for fusion with host cell, respectively (Wu et al., 2020). Fan Wu et al. revealed that the receptor-binding domain (RBD) of COVID-19 spike protein is fundamentally the same as that of SARS-CoVs (73.8–74.9% amino acid

CONTACT Asifkhan Shanavas asifkhan@inst.ac.in

character) and SARS-like CoVs, including strains Rs4874, Rs7327 and Rs4231 (75.9–76.9% amino acid) (Wu et al., 2020; Yuan et al., 2017). Peng Zhou et al. confirmed that SARS-CoV-2 uses human ACE2 receptor for cell entry (Q. Wang et al., 2020; P. Zhou et al., 2020) and this receptor can turn out to be a potential target to block the attachment of SARS-CoV-2 spike protein (Zhang et al., 2020). Among several viral proteins, the main protease of SARS-Cov2 (M^{pro}) is more potent target due to its vital role in the virus replication and transcription inside the host cells (Jin et al., 2020). As the novel coronavirus (SARS-CoV-2) have sequence homology with SARS and MERS thus the existing antiviral drugs seem effective against SARS-CoV-2. Remdesivir, a nucleotide analogue inhibitor of RdRp and antimalarial drug chloroquine effectively inhibited the SARS-CoV-2 infection *in vitro* (M. Wang et al., 2020). Hydroxychloroquine, an analogue of chloroquine is also a drug candidate after *in vitro* (Yao et al., 2020) and clinical investigations (Gautret et al. 2020). Considering the increase in fatality, there is an urgent requirement to channeled approved drugs and natural active compounds towards fighting the pandemic (Y. Zhou et al., 2020). This has led to several computational studies that screened hundreds of small molecules for their binding to key proteins such as spike glycoprotein, envelop protein, membrane protein and nucleocapsid protein (Das et al., 2020; Islam et al., 2020; Farag et al., 2020; Micael et al., 2020; Pandit et al., 2020; Ubani et al., 2020; Tallei et al., 2020; Romulo et al., 2020; Liu et al., 2020). As natural product repository has overwhelming number of leads that may act as both blocker of receptor mediated host cell uptake of the viral particles and inhibitor of the viral replication. In this direction, we have selected two target proteins (viral protein, M^{pro} and host receptor protein, ACE2) and performed docking studies to screen potential natural products. Further, *in silico* ADME (Absorption, Distribution, Metabolism, Excretion) analysis has been performed to understand their suitability as a drug candidate. While the top leads, Delphinidin 3,5-diglucoside, Scutellarein 7-glucoside, Avicularin and 3,5-Di-O-galloylshikimic acid show optimal binding at the active site of both SARS-CoV-2 M^{pro} and ACE2, ADME calculations show that all these molecules have low bioavailability.

Material and methods

Target selection

We selected viral and host targets, SARS CoV-2 main protease (Mpro) and ACE2, respectively to identify effective leads. Mpro is a homodimer with two protomers, each containing three domains (I, II and III) and a CYS-HIS catalytic dyad inside the cleft between domain I and II. This cleft has four subsites (S1, S1′, S2 and S4) that remain conserved in all coronavirus Mpro. The other target is a host protein, ACE2 (angiotensin-converting enzyme-related carboxypeptidase) which is having HEXXH-E zinc-binding consensus sequence. Extracellular region of ACE2 consist of two domains (I and II), a zinc metallopeptidase (residues 19–611) and C terminus (residues 612–740). Zinc metallopeptidase further have two domains in which catalytic site for ACE2 inhibitors is present. Along with the presence of residues coordinating with the zinc the catalytic site also have two subsites S1 and S1′ defined by specific residues which occupies major portion providing substrate binding specificity (Towler et al., 2004).

Molecular docking and natural products screening

Molecular docking was performed, using glide package of Schrödinger chemical simulation software (Schrödinger, LLC, and New York, NY). The crystal structure of SARS-Cov-2 M^{pro} and ACE2 was sourced from PDB data bank (PDB-ID: 6lu7 (Jin et al., 2020), 1R4L (Towler et al., 2004)). The protein preparation wizard was utilized to preprocess the crystal structure which includes removal of water molecules present beyond 5 Å, addition of right bond order, addition of H-atoms and optimization of hydroxyl and amino groups. Restrained minimization was performed using OPLS3 force field until the average root mean square deviation of the non-hydrogen atoms reached 0.3 Å. The receptor grid generation module was employed to generate grid for M^{pro} and ACE2 co-crystallized with its inhibitors, N3 and MLN4760, respectively. Position of N3 and MLN-4760 was set as the primary active site for the docking of selected ligands. The size of protein grid was optimized by re-docking of co-crystallized ligand within RMSD value < 2 Å. Up to 55 molecules (Source: PUBchem) were imported to the LigPrep module of Schrödinger software package to generate possible ionization states at the pH range 7 ± 2 using Epik. Up to 60 conformers were generated for single ligand and chirality was determined from the 3D structure. The generated conformers of all the screened ligands were docked to the M^{pro} using extra precision mode.

MM-GBSA dG binding energy calculations

On the basis of binding interaction energies ligand-protein complexes were re-scored by using MM-GB/SA (molecular mechanics energies combined with generalized born and surface area) module of Schrödinger software to enhance the binding affinity predictions.

ADME parameters calculations

It is vital to explore the pharmacokinetic profile of a molecule to be eligible as an active drug in clinical trial. The druggability of screened molecules were investigated for ADME properties using Swiss ADME software (Daina et al., 2017). Three pharmacokinetic parameters (Lipophilicity, solubility and bioavailability) were considered for the purpose of handling and formulation. Lipophilicity (Log P) calculations were based on XLOGP3 model (Cheng et al., 2007) and solubility calculation was based on ESOL model (Delaney, 2004), while bioavailability scores were based on the method developed by Martin (2005).

Results and discussion

SARS CoV-2 main protease (M^{pro}) and ACE2 were used as target to identify effective leads. M^{pro} processes polyproteins into 16 non-structural proteins (NSPs), which further generates subgenomic RNAs encoding for four main structural proteins (envelope (E), membrane (M), spike (S) and nucleocapsid (N) proteins) and other additional proteins (Coleman et al., 2014; Lu et al., 2020; Roh, 2012). In the S1 subsite of M^{pro}, GLN is vital for high cleavage efficiency and is specific to this particular protease. There is no known M^{pro} human homolog with similar cleavage site making it an interesting antiviral target with lower probability of inhibitor toxicity. While human ACE2 belongs to the category of type I integral membrane protein having 805 amino acids. Despite its role in making a pathway for SARS-CoV2 (Q. Wang et al., 2020), ACE2 prevents lung injuries, resulting in worsening of pathological condition (Zhang et al., 2020).

The catalytic sub domain of human ACE2 in presence of inhibitor undergoes hinge bending movement causing the deep cleft of the subdomain I of enzyme to wrap the inhibitor. This closing of subdomain I around inhibitor changes the conformation of the whole receptor making it less susceptible to interact with SARS-CoV2 receptor binding domain. In the free form zinc makes coordination bonds with three residues (HIS^{374}, HIS^{378} and GLU^{402}) and a water molecule (Towler et al., 2004). The leads are explored under two key categories (a) drug candidates undergoing clinical evaluation and (b) natural products (Arts et al., 2004; McGhie & Walton, 2007; Okonogi et al., 2016; Paul et al., 2018; Stenlid, 1976; Yuldashev, 2002) (Table 1). Glide (Friesner et al., 2004) Extra Precision (XP) approach was used for screening of candidates followed by calculation of MM-GBSA energies to increase accuracy, and reliability of the docking process. The SARS-CoV2 M^{pro} crystal structure plays an important role in identifying lead drugs through molecular simulation studies. The crystal structure sourced from protein databank has co-crystallized ligand N3, a michael acceptor that act as an irreversible inhibitor (Jin et al., 2020). To validate the methods utilized in this work, N3 was re-docked to its active site in M^{pro} (RMSD value < 2 Å). The docking yielded similar binding interactions as reported by Zhenming et al. and the MM-GBSA binding energy for N3 was calculated to be -80 Kcal/mol. The lactam of N3 embeds into the S1 subsite and forms a hydrogen bond with H^{163} as reported earlier. Also, N3 forms multiple hydrogen bonds with the residues in the substrate-binding pocket. The docking pose is presented in Figure 1(i). On the other hand the crystal structure of human ACE2 (PDB ID: 1R4l) Figure 2(i) bound with its inhibitor (MLN-4760) was also validated by re-docking. The residues involved in the binding site showed similar interaction as reported by Towler et al. with the docking score of -10.74 Kcal/mol and MM-GBSA score of -51.79 Kcal/mol. ACE2 behaves differently with or without the inhibitor. In the presence of its inhibitor subdomain I of zinc matallopeptidase undergo conformational change which could prevents the binding of SARS-CoV2 to its surface.

Further we attempted to dock GS-441524 (active form of remdesivir) and hydrochloroquine, which are being repurposed for treating COVID-19. The rational for including these molecules is that their principle inhibitory mechanism takes place inside the host cell where viral replication unfolds. The possibility for these molecules to bind to off-target proteins that are of viral or host origin cannot be ruled out. Recently FDA has issued an Emergency Use Authorization (EUA) for remdesivir to be included in treatment protocol of hospitalized SARS-CoV-2 infected patients (Rhoades, 2020).

Remdesivir is a prodrug of adenosine triphosphate (ATP) analog, GS-441524 that interferes with the action of viral RNA-dependent RNA polymerase towards controlling viral RNA production. From the present study, the estimated docking scores and MM-GBSA bind energies for GS-441524 are -6.24 Kcal/mol and -46.51 Kcal/mol for Mpro and -5.65 Kcal/mol and -40.48 Kcal/mol for ACE2, respectively. For SARS-CoV2 M^{pro} the docked poses of GS-441524 shows the hydroxyl groups of oxolan ring are inserted inside the S1 subunit by multiple hydrogen bonds with the CYS^{145} and ASN^{142}. The nitrogen of the nitrile group was found to form a hydrogen bond with the GLU^{166} of the side chain of S1 subunit. However for ACE2 multiple hydrogen bonds were formed by hydroxyl groups of the oxolane ring with PRO^{346}, ARG^{273} of S1 subsite, and ARG^{518} of the side chain. The oxygen of the oxolane ring was found forming hydrogen bond with the THR371 residue of the side chain. The free amine group interacts with the ASP^{367} residue of the S1′ subsite through hydrogen bonding. Non-specific binding to M^{pro} might be also contribute to the overall CoV inhibitory potential of the drug, which has shown encouraging results in terms of reduced time to clinical recovery but with insignificant clinical benefits in COVID-19 patients. However, further *in vitro* target-ligand interaction studies are required to assess concentration dependence of its inhibitory effect via M^{pro} binding. Similar to remdesivir, Hydroxychloroqine has also been assigned for EUA from FDA (2020) to treat hospitalized, severely ill SARS-CoV2 infected patients.

The MM-GBSA binding energy for HCQ with M^{pro} and ACE2 was found to be -67.53 Kcal/mol and -59.03 Kcal/mol. In the M^{pro} catalytic site it forms π-π stacking interaction between quinolin and HIE^{41} of the hydrophobic S2 subunit. The hydrogen of the two amine groups was showing interaction with the GLN^{189} and CYS^{145} through hydrogen bond and non-covalent ionic interaction (salt bridge). The hydroxyl group of the alkyl chain was found to interact through hydrogen bond with GLY^{143} residue of the S1 subunit. While this drug shows good binding to M^{pro} catalytic site, it is also labeled for possible cardiac injury (FDA, 2020). While in the catalytic site of ACE2 the free hydroxyl group of alkyl chain and the hydrogen of tertiary amine group interact with the side chain residue ASP^{367} through hydrogen bonds and one non-covalent ionic interaction was also formed between ASP^{367} and hydrogen of tertiary amine group. The side chain residue HIE^{345} was found to interact through couple of π-π stacking interaction with the two rings of quinolin nucleus. The 2D and 3D docking pose of both remdesivir and hydroxychloroquine in SARS-CoV-2 M^{pro} and ACE2 is presented in Figure 1(ii) and (iii) and Figure 2 (ii) and (iii).

Table 1. Docking scores of N3/MLN-4760 (1), drug candidates undergoing clinical trials (2a/b and 3) and potential natural compounds (4–7) against SARS-CoV2 M^{pro} (6LU7) and ACE2 (1R4L) and their ADME properties.

S.no	Leads	Docking score (Kcal/mol) 6LU7/1R4L	Lipophilicity (Log P)	Solubility (Log S)	Bioavailability score	MM-GBSA dG bind (Kcal/mol)
1.	N3/MLN-4765 (Co-crystallized inhibitors of M^{pro}/ACE2)	−8.93/−10.74	2.22	−3.77	0.17*	−80.27/−51.79
2a.	Remdesivir	−8.21/ −6.42	1.91	−4.12	0.17*	−71.68/ −51.52
2b.	GS-441524 (Active metabolite of Remdesivir)	−6.24/−5.65	−1.41	−0.94	0.55**	−46.51/−40.48
3.	Hydroxy-chloroquine	−7.11/−7.6	3.58	−3.91	0.55**	−67.53/ −59.03
4.	Delphinidin 3,5-diglucoside	−12.2/−13.6	−2.02	−2.27	0.17*	−74.0/−79.5
5.	Scutellarein 7-glucoside	−9.3/ −10.6	0.51	−3.05	0.17*	−68.55/ −59.1
6.	Avicularin	−9.6/ −8.0	0.98	−3.27	0.17*	−66.6/ −44.50
7.	3,5-Di-O-galloylshikimic acid	−10.3/ −11.2	0.61	−2.99	0.11*	−35.1/ −51.7

*Lipinski's rule – 2 violations.
**Passes Lipinski's rule.

Among the 30 natural secondary metabolites screened, the top four leads exhibiting highest binding affinity were re-scored for their MM-GB/SA dG bind energies and predict their docking poses (Guimarães & Cardozo, 2008). All these four natural secondary metabolites were found to fit perfectly at the active site pockets of SARS-CoV-2 M^{pro} and human ACE2. By analysis of the interactions it can be inferred that the active site of M^{pro} is polar in nature and shows good binding energies with ligands having polar functional groups. All the top four leads are presented in Table 1 with corresponding docking scores, MM-GB/SA dG bind energies, and pharmacokinetic descriptors for both the targets. For SARS-CoV-2 M^{pro}, similar to N3, the screened leads also engaged through multiple H-bond with the residues present in the cleft between domain I and II of M^{pro} of SARS-CoV-2. The key residues involved in the binding interaction are GLN^{166}, HIS^{163}, THR^{190}, CYS^{145}, GLN^{189} of main chain bonded through H-bonding and H41 of the hydrophobic pocket through π stacking interaction. Delphinidin 3,5-diglucoside is an anthocyanin mainly found in high concentration in pomegranates. It is a phenolic compound formed of anthocyanidin unit which is linked to carbohydrate moiety with O-glycoside at the C5-position. There are few reports on the therapeutic potential of this anthocyanin as an anticancer agent against colon and fibrosarcoma cancer. One of them reported that it significantly inhibited the HCT 116 and HT-29 human colon cancer cells (Mazewski et al., 2019). In another study, delphinidin-3,5-glucoside showed cytotoxicity in combination with other anthocyanins (gallic acid, delphinidin and pelargonidin3-glucosides) (Filipiak et al., 2014).

Present *in silico* analysis showed its highest binding affinity against for both the targets, M^{pro} and ACE2. The estimated docking scores were −12.2 Kcal/mol for M^{pro} and −13.6 Kcal/mol for ACE2 and MM-GBSA dG binding energies came out be −74 Kcal/mol and −79.47 Kcal/mol, respectively, which are lowest among all the screened ligands for both the targets. The 2D and 3D generated docking poses in M^{pro} (Figure 2(i)) shows that the hydroxyl groups of the glycone participate in H-bond interaction with GLU^{166} and ASN^{142} of the main chain, and with LEU^{141} of S1 subunit. The hydroxyl groups of benzene ring interact with CYS^{145} of the catalytic site and HIS^{164} of the S2 subunit through H-bond. Docking results also exposed the π-π interaction between the benzene ring and the HIE41 of the hydrophobic cavity of S2 subunit. The hydroxyl group of flavylium nucleus found to be interacting with the THR^{190} of S4 subunit. On the contrary 2D and 3D refined poses of delphinidin-3,5-glucoside (Figure 3(i)) in the catalytic site of ACE2 flag up pi-cation interaction between the rings of flavylium nucleus and the side chain residues ARG^{273} and HIE^{345} of the catalytic site. Flavylium rings were also showing π-π interaction with the residues HIE^{345} and $HIS^{374}$and its hydroxyl was bonded through hydrogen bond to the GLU^{375}. In addition to this the hydroxyls of the sugar moiety were found to have multiple hydrogen bond interaction with GLU406, THR371, ASH368, and ASP367. Likewise hydroxyls of the phenyl ring were bonded to TYR^{127} with multiple hydrogen bonds.

The second lead compound is a flavonoid glycoside, Scutellarein 7-glucoside isolated from plants like *Verbena officinalis L* (Rehecho et al., 2011), *Buddleja madagascariensis Lam* (Emam et al., 1998), *Plantago asiatica L*, *Scutellaria immaculate* (Yuldashev, 2002), *Plantago asiatica L* and *Polygonum odoratum* (Okonogi et al., 2016). Biologically scutellarein 7-glucoside shows anti-inflammatory activity by decreasing the IL-6 and TNF-α production as reported by Okonogi et al. (2016). Another study reported by Goran et al., shows its certain inhibitory activity against indole-3-acetic acid oxidase there by inhibiting ATP formation inside the plant mitochondria (Stenlid, 1976). In addition to these properties Rehecho et al. (2011) reported that it also shows free radical scavenging activity. The binding affinity docking scores of Scutellarein 7-glucoside against M^{pro} and ACE2 are −9.3 Kcal/mol and −10.6 Kcal/mol. The MM-GBSA dG binding energies are −68.55 Kcal/mol and −59.1 Kcal/mol. In M^{pro} all the hydroxyl groups of sugar moiety are involved in H-bonding with the CYS^{145}, His^{163} and GLU^{166} which are the main residues of the catalytic site. Moreover hydroxyl group of phenyl ring also interacts with the GLN^{192} residue of S4 subunit through hydrogen bonding that further secures scutellarein 7-glucoside binding to M^{pro} (Figure 3(ii)). While in case of the ACE2 enzyme the hydroxyls of the sugar moiety were locking the Scutellarein 7-glucoside by forming multiple hydrogen bonds with GLU^{375}, HIE^{345} and HIE^{505}. The phenyl ring was shown to make π-π stacking interaction with the phenyl ring of HIE^{345}. The carbonyl oxygen and hydroxyl group of chromone nucleus were displaying hydrogen bond interaction with the THR^{371} and ASH^{368} (Figure 4(ii)).

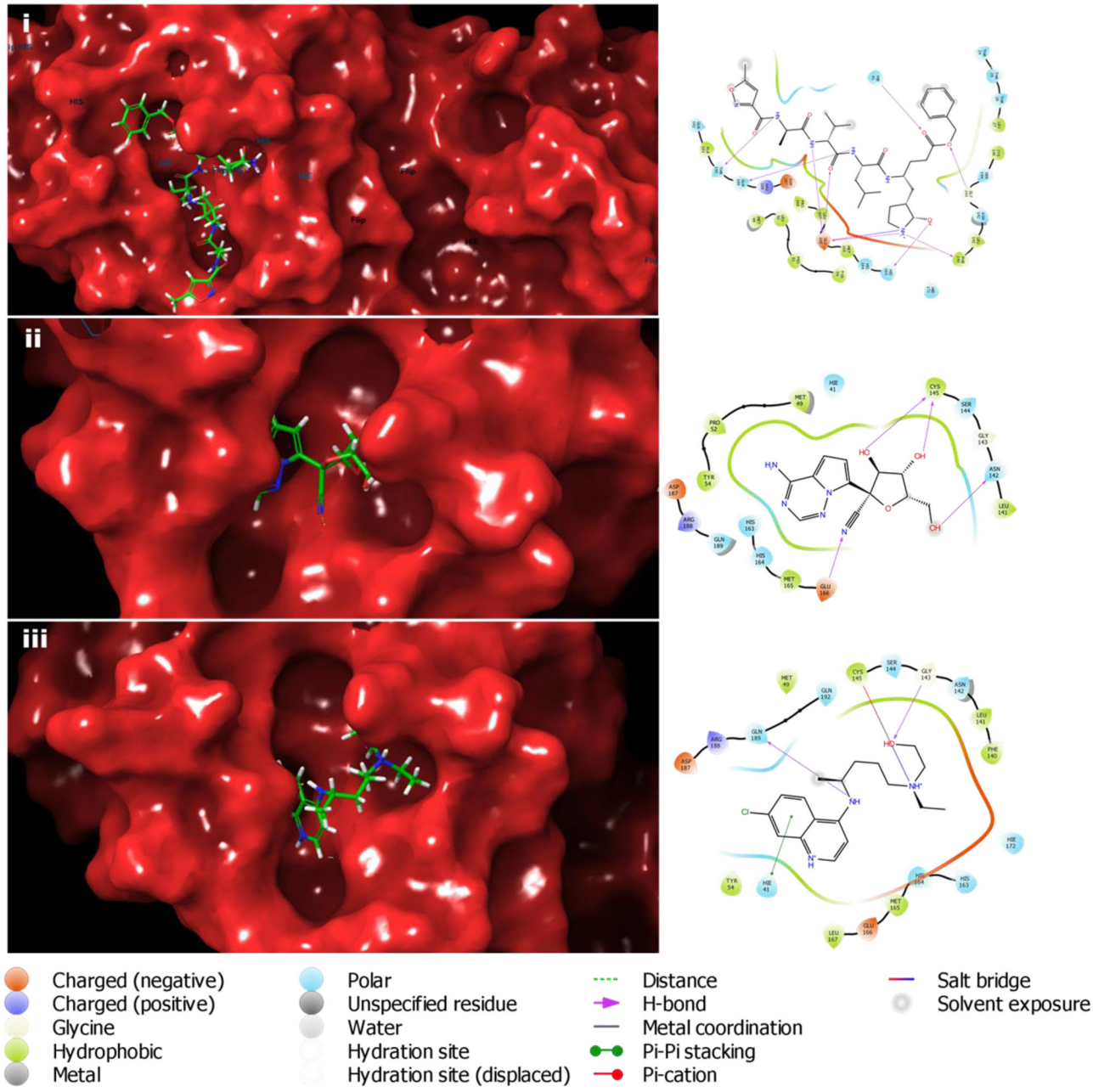

Figure 1. Docked pose and binding interactions of N3 (i), GS-441524 (ii) and Hydroxychloroquine (iii) with SARS-Cov-2 M^{pro}.

Avicularin is a flavonoid isolated from *Polygonum aviculare, Rhododendron aureum and Taxillus kaempferi* (Fukunaga et al., 1989; Zhang et al., 1989). A derivative of quercetin, it possesses biological properties including anti-cancer, anti-inflammatory, anti-oxidant, anti-allergic properties. Van Anh Vo et al., demonstrated the anti-inflammatory activity of avicularin by LPS-induced suppression of ERK signaling pathway in RAW 264.7 macrophage cells (Determination of Avicularin in Polygonum Aviculare L. by Square Wave Polarography. - PubMed - NCBI, n.d.). Avicularin elevated the sensitivity of cisplatin in drug resistant gastric cancer cells in *in vitro* and *in vivo* studies by enhancing the Bax and Bak expressions (Guo et al., 2018). In another study, avicularin suppressed the intracellular accumulation of lipids by suppressing C/EBPα-mediated activation of GLUT4 expression in 3T3-L1 cells (Fujimori & Shibano, 2013). Present computational analysis showed that it has good affinity to M^{pro} with a docking score of −9.6 Kcal/mol and MM-GBSA dG binding energy −66.6 Kcal/mol. Similar to Delphinidin 3,5-diglucoside and scutellarein 7-glucoside, the alpha-L-arabinofuranosy moiety of avicularin is majorly involved in interaction with the main residues (CYS^{145} and GLU^{166}) of the catalytic site via hydrogen bonding. To further increase the binding affinity, the benzene ring forms π-π stacking with the HIE^{41} of the hydrophobic subsite. Also the hydroxyl group of chromone nucleus and benzene ring were found to interact with the THR^{190} and HIS^{164}, CYS^{145}, respectively through hydrogen bonding, enhancing the fit into the active site (Figure 3(iii)). On the other hand avicularin has highest MM-GBSA dG binding energy of −44.50 Kcal/mol among all top leads for ACE2

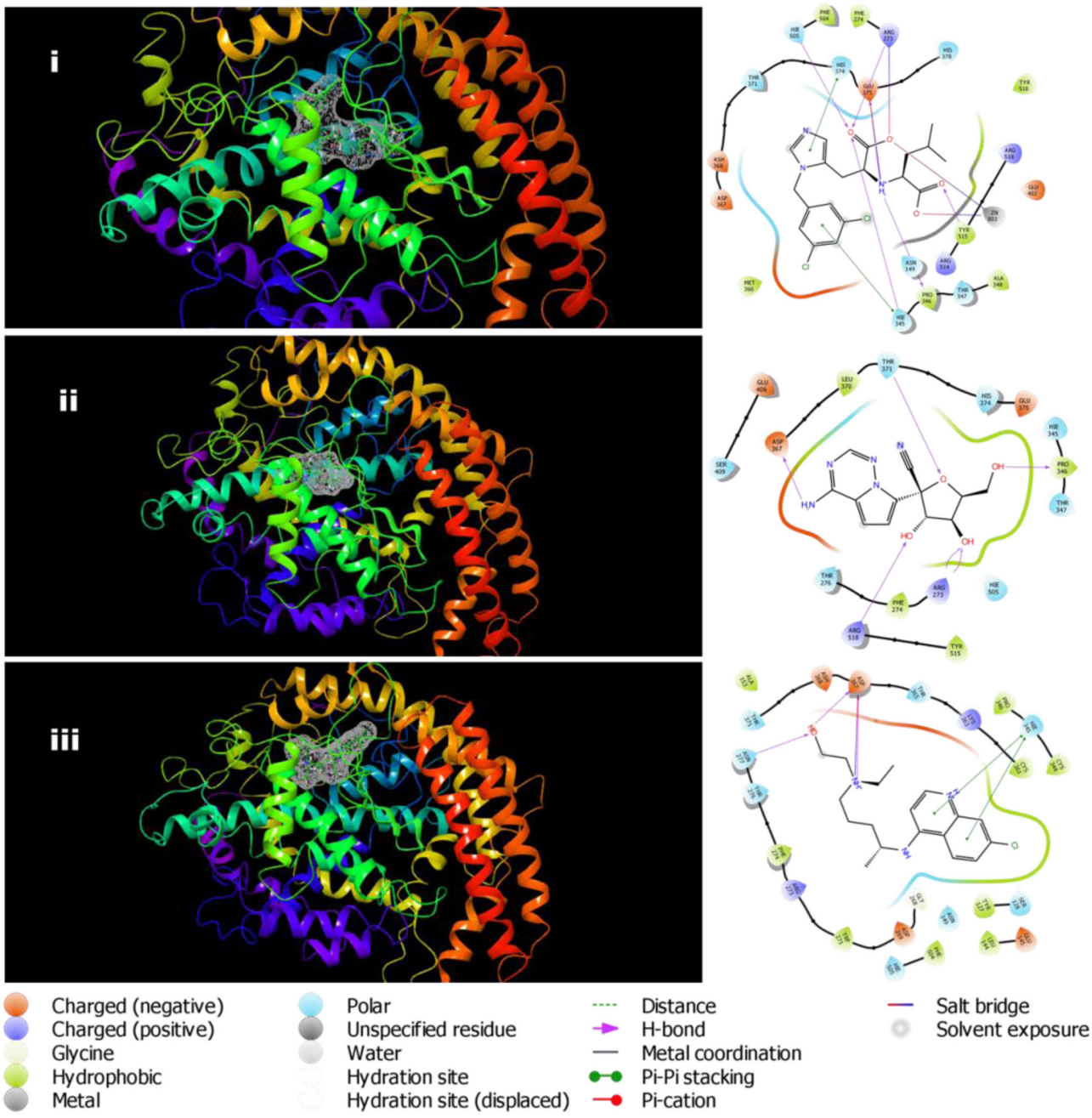

Figure 2. Docked pose and binding interactions of MLN-4765 (i), GS-441524 (ii) and Hydroxychloroquine (iii) with ACE2.

enzyme. The hydroxyls of the alpha-L-arabinofuranosy moiety and phenyl ring shows binding interaction with residues GLU^{406}, THR^{445}, ASP^{367} and ASH^{368} of domain I. Docking poses also reveals the presence of multiple π-cation interaction between chromone nucleus and ARG^{273}. The carbonyl group of main nucleus was found to be bonded with ARG^{518} through hydrogen bonding (Figure 4(iii)).

Out of top 4 screened leads 3,5-Di-O-galloylshikimic acid have the highest MM-GBSA dG binding energy of −35.09 Kcal/mol with docking score of −10.3 kcal/mol for M^{pro}. It is also the only lead among top four that lacks a sugar moiety. To fit inside the M^{pro} cavity, the hydroxyl groups of benzoyl moiety are involved in H-bonding with the S4 subsite residues (THR^{190}), and S1 subsite residues (HIS^{163}, ASN^{142}). The hydroxyl group and the oxygen atoms of both the benzoyl groups are found to interact with the LEU^{167}, GLY^{143} and GLU^{166} (Figure 3(iv)).

However for ACE2, 3,5-Di-O-galloylshikimic acid has the 3rd lowest MM-GBSA dG binding energy of −51.7 Kcal/mol with docking score of −11.16 kcal/mol. From the docked poses inside ACE2 catalytic site, it can be concluded that oxygen of the carboxylate was found to interact with HIE^{505} and HIE^{345} through hydrogen bonding and with ARG^{273} through non-covalent ionic interaction (salt bridge). The hydroxyls of the benzoyl moiety were displaying hydrogen bonding interaction with the TYR^{127} and GLU^{406}. HIE^{345} of the side chain was involved in the π-π stacking interaction with one of the benzoyl ring (Figure 4(iv)). The docking score of all the screened natural secondary metabolites is shown in Figure 5.

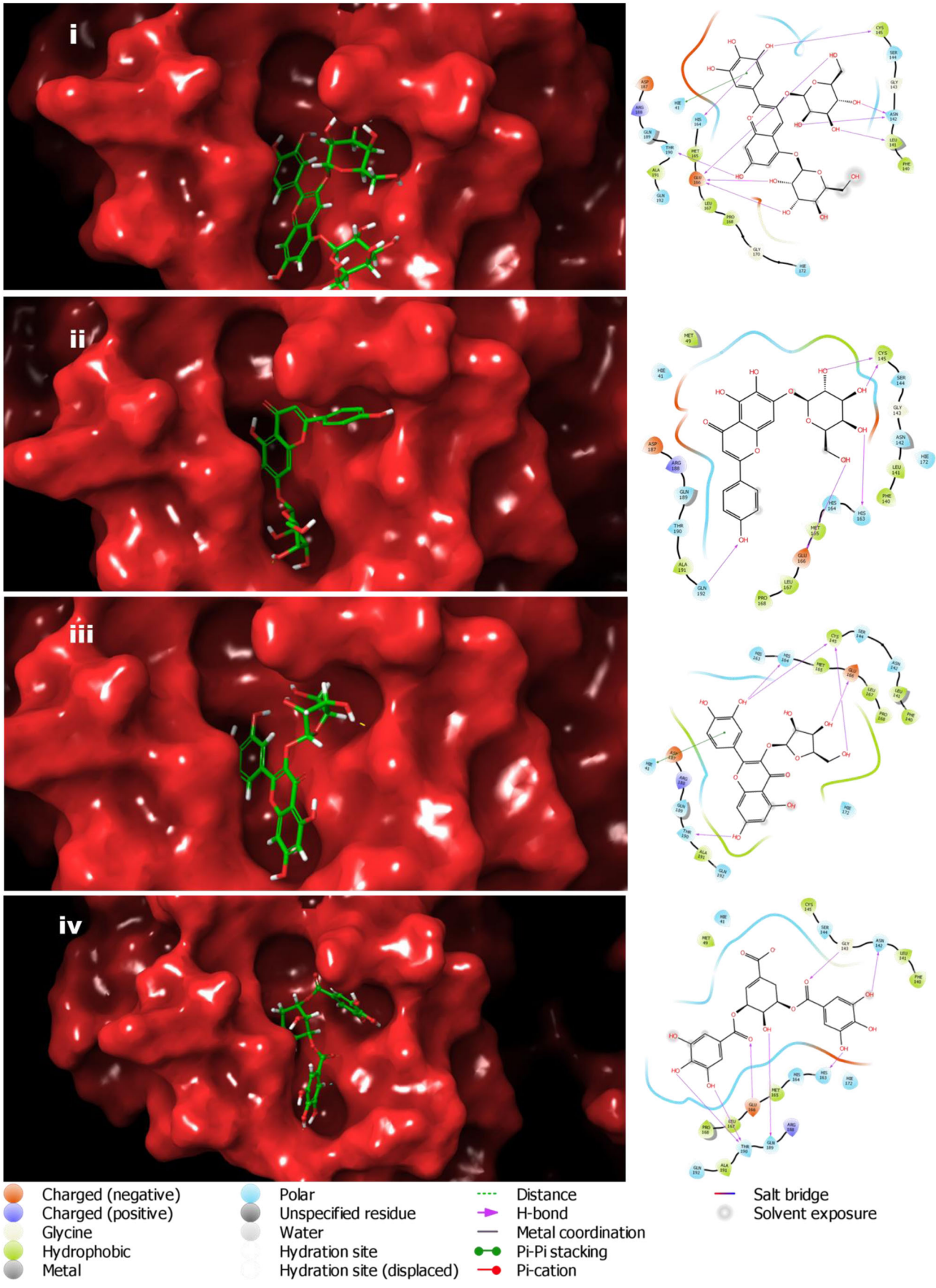

Figure 3. Docked pose and binding interactions of Delphinidin 3, 5-diglucoside (i), Scutellarein 7-glucoside (ii), Avicularin (iii) and 3,5-Di-O-galloylshikimic acid (iv) with SARS-Cov-2 M^{pro}.

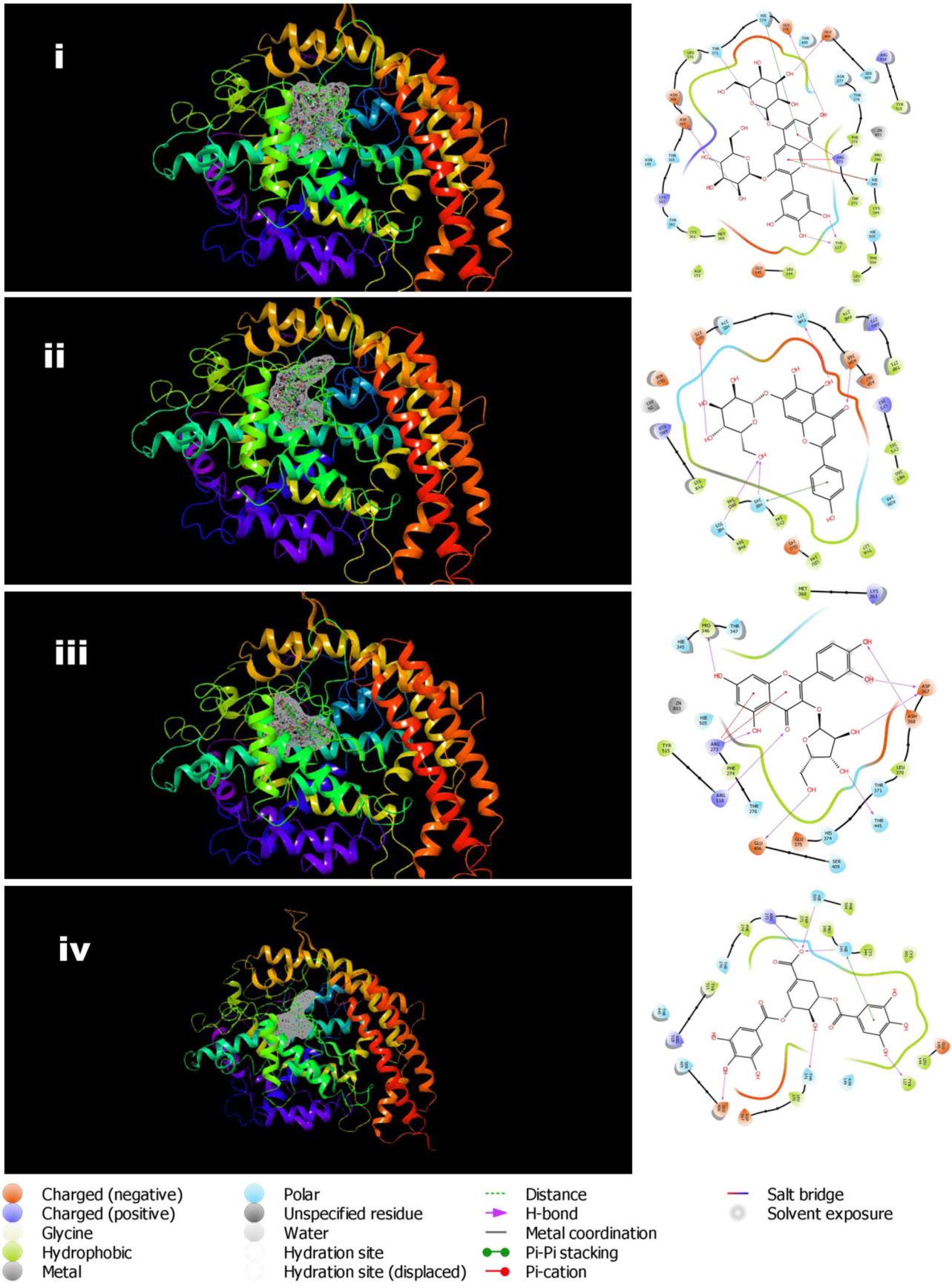

Figure 4. Docked pose and binding interactions of Delphinidin 3, 5-diglucoside (i), Scutellarein 7-glucoside (ii), Avicularin (iii) and 3,5-Di-O-galloylshikimic acid (iv) with ACE2.

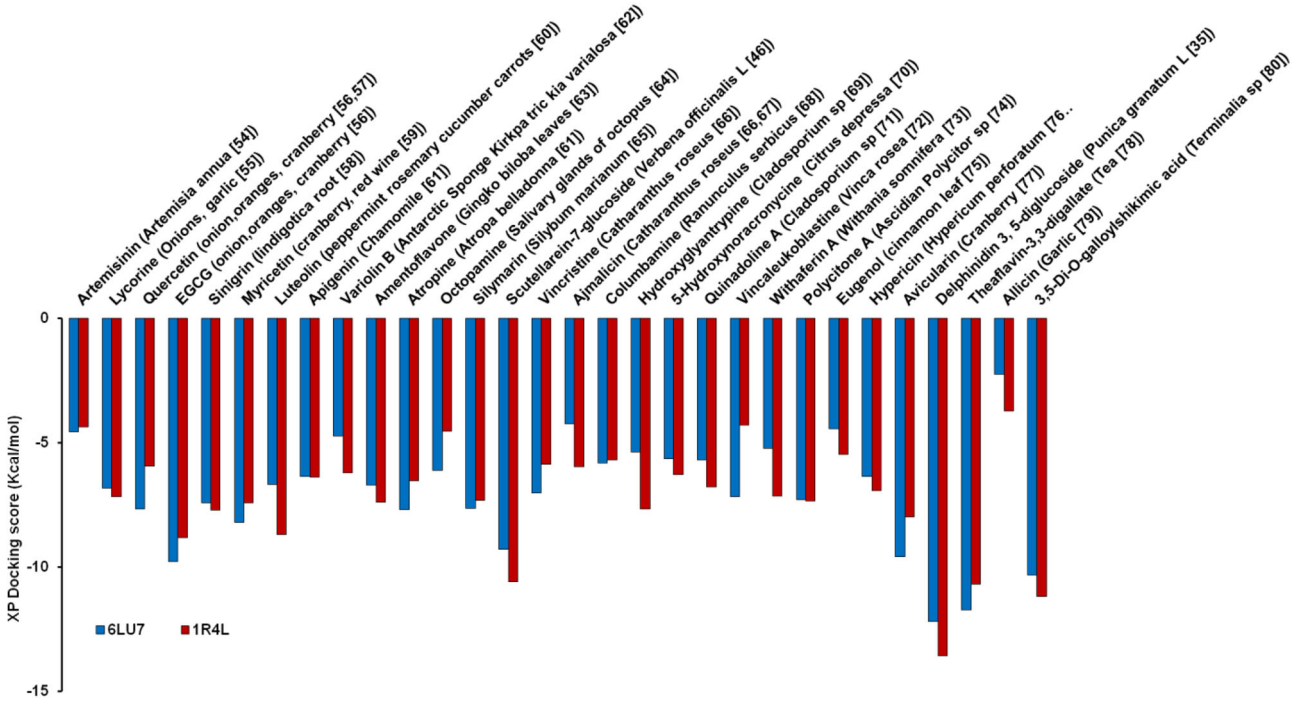

Figure 5. Docking scores of screened natural ligands. Parentheses contain (Source of the natural product [reference]).

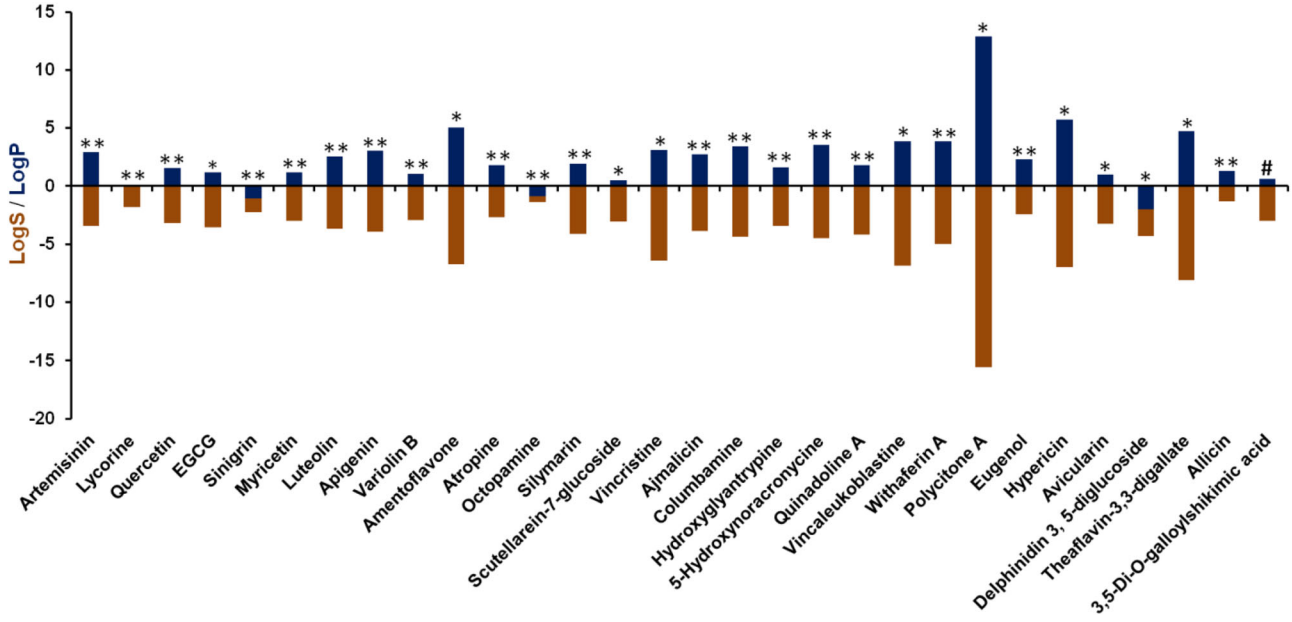

Figure 6. ADME properties of screened natural ligands. ABS = 0.11# or 0.17* or 0.55**.

To be eligible for clinical evaluation, pharmacokinetic profile of a drug plays pivotal role. Based on the results of ADME calculations all the investigated leads have low bioavailability score. The bioavailability score (ABS) depends on passing or violating Lipinski's rule of five. At biological pH, a compound is expected to have >10% bioavailability (F) in rat only if it pass Lipinski's rule of five with ABS 0.55 (i.e. 55% chances of $F > 10\%$ in rat). However if it fails, ABS is only 0.17 i.e. 17% chance for a molecule to have bioavailability >10% in rat (Martin, 2005). With ABS-0.17, delphinidin 3,5-diglucoside (an anthocyanin), the bioavailability through gastro intestinal tract (GIT) is reported to be very low. A study reported by McGhie and Walton (2007) concluded that in animals and humans low anthocyanins levels are absorbed in the circulation and excreted in urine, but high levels are found in the gastrointestinal (GI) tract. Another investigation by Paul et al. (2018) suggests that anthocyanins in the form of crude extract have less bioavailability as compared to encapsulated spray dried formulations. Like delphinidin 3,5-diglucoside the next two leads (Scutellarein 7-glucoside, Avicularin) which are glycosidic flavonoids also have less bioavailability with acceptable water solubility limit. Glycosidic flavonoids show less permeability through GIT (Arts et al., 2004). Hollman et al. reported that only aglycone part of

flavonoids pass through the intestinal membrane and glycone moiety mostly gets digested in the GIT with time to reach peak concentrations (T_{max}) between <0.5 and 9 h (Walle, 2004). The 3,5-Di-O-galloylshikimic acid (gallotanin with quinic acid core) estimated log S value suggest that it has acceptable water solubility due to presence of polar functional groups, yet its bioavailability score is only 0.11.

Both from docking and ADME analysis, it is clear that the sugar moieties and other polar groups are both responsible for the high binding affinity to M^{pro}/ACE2 and low oral bioavailability. Among other natural compounds reported to bind with M^{pro} and ACE2, Epigallocatechin gallate (EGCG) (Khaerunnisa et al., 2020; Lalit & Vyomesh, 2020; Mittal et al., 2020) and Theaflavin-3,3-digallate (Manish, 2020) also showed very good binding to M^{pro} and ACE2, but has poor oral bioavailability (ABS-0.17) (Figure 6). Specifically, EGCG has been reported to be broken down in large intestine by the colonic microflora. The fraction of EGCG that is absorbed might undergo rapid methylation catalyzed by liver cytosolic catechol-*O*-methyltransferase which decreases its hydrophilicity (Mereles & Hunstein, 2011), the key feature found responsible for M^{pro} inhibition. Thus a majority of the natural molecules with therapeutic potential against SARS-CoVs require an effective way to get delivered to lung in their native form to bypass degradation and metabolism associated with oral route.

Conclusion

Traditional medicines in different countries have history of successfully treating several epidemics and endemics. With advanced drug discovery tools in place, it is feasible to screen active ingredients of these natural concoctions for potential antiviral application. We attempted to explore this approach by screening selected natural secondary metabolites for their dual binding potential to (1) viral main protease M^{pro} that has a conserved catalytic cleavage site responsible for post-translational processing of polyproteins required for viral replication in all SARS corona viruses and (2) ACE2 the principle receptor responsible for entry of the viral particles into the host cells. The top four leads Delphinidin 3,5-diglucoside, Scutellarein 7-glucoside, Avicularin and 3,5-Di-O-galloylshikimic acid showed encouraging binding affinity with MM-GBSA energies up to −74.0 Kcal/mol and −79.5 Kcal/mol to M^{pro} and ACE2, respectively. However, their theoretical bioavailability score (ABS) of 0.11 or 0.17 makes them ineffective via oral route. Potential natural leads such as Delphinidin 3, 5-diglucoside, an anthocyanin responsible for the red pigmentation of pomegranate juice, are ingested orally. Nonetheless, their viral inhibitory potential is greatly limited by low oral bioavailability. To overcome this bottleneck, these molecules can be either engineered to withstand GIT degradation and first pass metabolism or can be encapsulated in nano/microparticles towards their site specific pulmonary delivery.

Acknowledgements

PS is thankful for JRF fellowship received under DBT funded project under Nanobiotechnology scheme (BT/PR21972/NNT/28/1280/2017). AS acknowledge the Government of India for funding under DST-SERB core research grant scheme (EMR/2016/003851). The authors sincerely acknowledge the support received from NIPER, S.A.S Nagar in performing molecular docking studies. AS thank Dr.Victor Arokia Doss (Associate Professor, Dept of Biochemistry) and Late. Dr.N.Abitha Devi (Ex-HoD, Dept of Biochemistry), PSG College of Arts and Science for mentorship and support.

Disclosure statement

No potential conflict of interest was reported by the authors.

ORCID

Asifkhan Shanavas http://orcid.org/0000-0001-7221-7477

References

Farag, A., Wang, P., Ahmed, M., and Sadek, H. (2020). Identification of FDA Approved Drugs Targeting COVID-19 Virus by Structure-Based Drug Repositioning (Version 2). https://doi.org/10.26434/CHEMRXIV.12049647.V1.

Arts, I. C. W., Sesink, A. L. A., Faassen-Peters, M., & Hollman, P. C. H. (2004). The type of sugar moiety is a major determinant of the small intestinal uptake and subsequent biliary excretion of dietary quercetin glycosides. *The British Journal of Nutrition*, *91*(6), 841–847. https://doi.org/10.1079/BJN20041123

Cheng, T., Zhao, Y., Li, X., Lin, F., Xu, Y., Zhang, X., Li, Y., Wang, R., & Lai, L. (2007). Computation of octanol-water partition coefficients by guiding an additive model with knowledge. *Journal of Chemical Information and Modeling*, *47*(6), 2140–2148. https://doi.org/10.1021/ci700257y

Coleman, C. M., Liu, Y. V., Mu, H., Taylor, J. K., Massare, M., Flyer, D. C., Glenn, G. M., Smith, G. E., & Frieman, M. B. (2014). Purified coronavirus spike protein nanoparticles induce coronavirus neutralizing antibodies in mice. *Vaccine*, *32* (26), 3169–3174. https://doi.org/10.1016/j.vaccine.2014.04.016

Daina, A., Michielin, O., & Zoete, V. (2017). SwissADME: A free web tool to evaluate pharmacokinetics, drug-likeness and medicinal chemistry friendliness of small molecules. *Scientific Reports*, *7*, 42717–42713. https://doi.org/10.1038/srep42717

Das, S., Sarmah, S., Lyndem, S., & Roy, A. S. (2020). An investigation into the identification of potential inhibitors of SARS-CoV-2 main protease using molecular docking study. " *Journal of Biomolecular Structure and Dynamics*, May, 1–11. https://doi.org/10.1080/07391102.2020.1763201.

Delaney, J. S. (2004). ESOL: Estimating aqueous solubility directly from molecular structure. *Journal of Chemical Information and Computer Sciences*, *44*(3), 1000–1005. https://doi.org/10.1021/ci034243x

Emam, A. M., R. Elias, A. M. Moussa, R. Faure, L. Debrauwer, and G. Balansard. (1998). Two Flavonoid Triglycosides from Buddleja Madagascariensis. *Phytochemistry, 48*(4), 739–42. https://doi.org/10.1016/S0031-9422(97)01043-1.

FDA. (2020). Hydroxychloroquine fact sheet for health care providers, 1–7.

Filipiak, K., Hidalgo, M., Silvan, J. M., Fabre, B., Carbajo, R. J., Pineda-Lucena, A., Ramos, A., De Pascual-Teresa, B., & De Pascual-Teresa, S. (2014). Dietary gallic acid and anthocyanin cytotoxicity on human fibrosarcoma HT1080 cells. A study on the mode of action. *Food & Function*, *5*(2), 381–389. https://doi.org/10.1039/c3fo60465a

Friesner, R. A., Banks, J. L., Murphy, R. B., Halgren, T. A., Klicic, J. J., Mainz, D. T., Repasky, M. P., Knoll, E. H., Shelley, M., Perry, J. K., Shaw, D. E., Francis, P., & Shenkin, P. S. (2004). Glide: A new approach for rapid, accurate docking and scoring. 1. Method and assessment of docking accuracy. *Journal of Medicinal Chemistry*, *47*(7), 1739–1749. https://doi.org/10.1021/jm0306430

Fujimori, K., & Shibano, M. (2013). Avicularin, a plant flavonoid, suppresses lipid accumulation through repression of C/EBPα-activated

GLUT4-mediated glucose uptake in 3T3-L1 cells. *Journal of Agricultural and Food Chemistry*, *61*(21), 5139–5147. https://doi.org/10.1021/jf401154c

Fukunaga, T., Nishiya, K., Kajikawa, I., Takeya, K., & Itokawa, H. (1989). Studies on the constituents of Japanese mistletoes from different host trees, and their antimicrobial and hypotensive properties. *Chemical & Pharmaceutical Bulletin*, *37*(6), 1543–1546. https://doi.org/10.1248/cpb.37.1543

Gautret, P., Lagier, J.-C., Parola, P., Hoang, V. T., Meddeb, L., Mailhe, M., Doudier, B., Courjon, J., Giordanengo, V., Vieira, V. E., Dupont, H. T., Honoré, S., Colson, P., Chabrière, E., La Scola, B., Rolain, J.-M., Brouqui, P., & Raoult, D. (2020). Hydroxychloroquine and azithromycin as a treatment of COVID-19: Results of an open-label non-randomized clinical trial. *International Journal of Antimicrobial Agents*, 105949. https://doi.org/10.1016/j.ijantimicag.2020.105949

Guimarães, C. R. W., & Cardozo, M. (2008). MM-GB/SA rescoring of docking poses in structure-based lead optimization. *Journal of Chemical Information and Modeling*, *48*(5), 958–970. https://doi.org/10.1021/ci800004w

Guo, X. F., Liu, J. P., Ma, S. Q., Zhang, P., & De Sun, W. (2018). Avicularin reversed multidrug-resistance in human gastric cancer through enhancing Bax and BOK expressions. *Biomedicine & Pharmacotherapy = Biomedecine & Pharmacotherapie*, *103*, 67–74. https://doi.org/10.1016/j.biopha.2018.03.110

Hu, D., Zhu, C., Ai, L., He, T., Wang, Y., Ye, F., Yang, L., Ding, C., Zhu, X., Lv, R., Zhu, J., Hassan, B., Feng, Y., Tan, W., & Wang, C. (2018). Genomic characterization and infectivity of a novel SARS-like coronavirus in Chinese bats. *Emerging Microbes & Infections*, *7*(1), 1–10. https://doi.org/10.1038/s41426-018-0155-5

Islam, R., Parves, R., Paul, A. S., Uddin, N., Rahman, M. S., Mamun, A. A., Hossain, M. N., Ali, M. A., & Halim, M. A. (2020). A molecular modeling approach to identify effective antiviral phytochemicals against the main protease of SARS-CoV-2. *Journal of Biomolecular Structure & Dynamics*, 1–20. https://doi.org/10.1080/07391102.2020.1761883.

Jin, Z., Du, X., Xu, Y., Deng, Y., Liu, M., Zhao, Y., Zhang, B., Li, X., Zhang, L., Peng, C., Duan, Y., Yu, J., Wang, L., Yang, K., Liu, F., Jiang, R., Yang, X., You, T., Liu, X., … Yang, H. (2020). Structure of Mpro from COVID-19 virus and discovery of its inhibitors. *Nature*, *582*(7811), 289–293. . https://doi.org/10.1038/s41586-020-2223-y

Khaerunnisa, S., Kurniawan, H., Awaluddin, R., & Suhartati, S. (2020). Potential inhibitor of COVID-19 main protease (M pro) from several medicinal plant compounds by molecular docking study. Preprints, 1–14. https://doi.org/10.20944/preprints202003.0226.v1.

Lalit, S., & Vyomesh, J. (2020). Comparative docking analysis of rational drugs against COVID-19 main protease. ChemRxiv. https://doi.org/10.26434/chemrxiv.12136002.v1.

Liu, H., Ye, F., Sun, Q., Liang, H., Li, C., Lu, R., Huang, B., Tan, W., & Lai, L. (2020). *Scutellaria baicalensis* extract and baicalein inhibit replication of SARS-CoV-2 and its 3C-like protease in vitro. BioRxiv, 2020.04.10.035824. https://doi.org/10.1101/2020.04.10.035824.

Lu, R., Zhao, X., Li, J., Niu, P., Yang, B., Wu, H., Wang, W., Song, H., Huang, B., Zhu, N., Bi, Y., Ma, X., Zhan, F., Wang, L., Hu, T., Zhou, H., Hu, Z., Zhou, W., Zhao, L., … Tan, W. (2020). Genomic characterisation and epidemiology of 2019 novel coronavirus: Implications for virus origins and receptor binding. *The Lancet*, *395*(10224), 565–574. https://doi.org/10.1016/S0140-6736(20)30251-8

Manish, M. (2020). Studies on computational molecular interaction between SARS-CoV-2 main protease and natural products. ChemRxiv, Preprint. https://doi.org/10.26434/chemrxiv.12024789.v1.

Martin, Y. C. (2005). A bioavailability score. *Journal of Medicinal Chemistry*, *48*(9), 3164–3170. https://doi.org/10.1021/jm0492002

Mazewski, C., Kim, M. S., & Gonzalez de Mejia, E. (2019). Anthocyanins, delphinidin-3-O-glucoside and cyanidin-3-O-glucoside, inhibit immune checkpoints in human colorectal cancer cells in vitro and in silico. *Scientific Reports*, *9*(1), 1–15. https://doi.org/10.1038/s41598-019-47903-0

McGhie, T. K., & Walton, M. C. (2007). The bioavailability and absorption of anthocyanins: Towards a better understanding. *Molecular Nutrition & Food Research*, *51*(6), 702–713. https://doi.org/10.1002/mnfr.200700092

Mereles, D., & Hunstein, W. (2011). Epigallocatechin-3-Gallate (EGCG) for clinical trials: More pitfalls than promises? *International Journal of Molecular Sciences*, *12*(9), 5592–5603. https://doi.org/10.3390/ijms12095592

Micael, D., de Oliveira, L., & de Oliveira Kelson Mota, T. (2020). Comparative computational study of SARS-CoV-2 receptors antagonists from already approved drugs. ChemRxiv. https://doi.org/10.26434/chemrxiv.12044538.v2.

Mittal, L., Kumari, A., Srivastava, M., Singh, M., & Asthana, S. (2020). Identification of potential molecules against COVID-19 main protease through structure-guided virtual screening approach. ChemRxiv, (1). Preprint. https://doi.org/10.26434/CHEMRXIV.12086565.V2.

Okonogi, S., Kheawfu, K., Holzer, W., Unger, F. M., Viernstein, H., & Mueller, M. (2016). Anti-inflammatory effects of compounds from Polygonum odoratum. *Natural Product Communications*, *11*(11), 1651–1654. https://doi.org/10.1177/1934578X1601101107

Pandit, M. n.d. In silico studies reveal potential antiviral activity of phytochemicals from medicinal plants for the treatment of COVID-19 infection. 1–38. https://doi.org/10.21203/rs.3.rs-22687/v1.

Paul, A., Banerjee, K., Goon, A., & Saha, S. (2018). Chemo-profiling of anthocyanins and fatty acids present in pomegranate aril and seed grown in Indian condition and its bioaccessibility study. *Journal of Food Science and Technology*, *55*(7), 2488–2496. https://doi.org/10.1007/s13197-018-3166-2

Rehecho, S., Hidalgo, O., García-Iñiguez de Cirano, M., Navarro, I., Astiasarán, I., Ansorena, D., Cavero, R. Y., & Calvo, M. I. (2011). Chemical composition, mineral content and antioxidant activity of Verbena officinalis L. *LWT - Food Science and Technology*, *44*(4), 875–882. https://doi.org/10.1016/j.lwt.2010.11.035

Rhoades, A. (2020). Remdesivir EUA letter of authorization. *564*, 1–6.

Roh, C. (2012). A facile inhibitor screening of SARS coronavirus N protein using nanoparticle-based RNA oligonucleotide. *International Journal of Nanomedicine*, *7*, 2173–2179. https://doi.org/10.2147/IJN.S31379

Rota, P. A., Oberste, M. S., Monroe, S. S., Nix, W. A., Campagnoli, R., Icenogle, J. P., Peñaranda, S., Bankamp, B., Maher, K., Chen, M.-H., Tong, S., Tamin, A., Lowe, L., Frace, M., DeRisi, J. L., Chen, Q., Wang, D., Erdman, D. D., Peret, T. C. T., … Bellini, W. J. (2003). Characterization of a novel coronavirus associated with severe acute respiratory syndrome. *Science*, *300*(5624), 1394–1399. https://doi.org/10.1126/science.1085952

Stenlid, G. (1976). Effects of substituents in the A-ring on the physiological activity of flavones. *Phytochemistry*, *15* (6), 911–912. https://doi.org/10.1016/S0031-9422(00)84368-X

Tallei, T., Tumilaar, S., Niode, N., Fatimawali, Kepel, B., Idroes, R. & Effendi, Y. (2020). Potential of plant bioactive compounds as SARS-CoV-2 main protease (Mpro) and spike (S) glycoprotein inhibitors: A molecular docking study. Preprints, no. 1–18. https://doi.org/10.20944/preprints202004.0102.v1.

Towler, P., Staker, B., Prasad, S. G., Menon, S., Tang, J., Parsons, T., Ryan, D., Fisher, M., Williams, D., Dales, N. A., Patane, M. A., & Pantoliano, M. W. (2004). ACE2 X-ray structures reveal a large hinge-bending motion important for inhibitor binding and catalysis. *The Journal of Biological Chemistry*, *279*(17), 17996–17997. https://doi.org/10.1074/jbc.M311191200

Ubani, A., Agwom, F., Shehu, N. Y., Luka, P., Umera, E. A., Umar, U., Omale, S., Nnadi, E., & Aguiyi, J. C. (2020). Molecular docking analysis of some phytochemicals on two SARS-CoV-2 targets. BioRxiv, 2020.03.31.017657. https://doi.org/10.1101/2020.03.31.017657.

Walle, T. (2004). Absorption and metabolism of flavonoids. *Free Radical Biology & Medicine*, *36*(7), 829–837. https://doi.org/10.1016/j.freeradbiomed.2004.01.002

Wang, M., Cao, R., Zhang, L., Yang, X., Liu, J., Xu, M., Shi, Z., Hu, Z., Zhong, W., & Xiao, G. (2020). Remdesivir and chloroquine effectively inhibit the recently emerged novel coronavirus (2019-NCoV) in vitro. *Cell Research*, *30*(3), 269–271. https://doi.org/10.1038/s41422-020-0282-0

Wang, Q., Zhang, Y., Wu, L., Niu, S., Song, C., Zhang, Z., Lu, G., Qiao, C., Hu, Y., Yuen, K.-Y., Wang, Q., Zhou, H., Yan, J., & Qi, J. (2020). Structural and functional basis of SARS-CoV-2 entry by using human ACE2. *Cell*, *181*(4), 894–904.e9. https://doi.org/10.1016/j.cell.2020.03.045

Wu, F., Zhao, S., Yu, B., Chen, Y.-M., Wang, W., Song, Z.-G., Hu, Y., Tao, Z.-W., Tian, J.-H., Pei, Y.-Y., Yuan, M.-L., Zhang, Y.-L., Dai, F.-H., Liu, Y.,

Wang, Q.-M., Zheng, J.-J., Xu, L., Holmes, E. C., & Zhang, Y.-Z. (2020). A new coronavirus associated with human respiratory disease in China. *Nature*, *579*(7798), 265–269. https://doi.org/10.1038/s41586-020-2008-3

Yao, X., Ye, F., Zhang, M., Cui, C., Huang, B., Niu, P., Liu, X., Zhao, L., Dong, E., Song, C., Zhan, S., Lu, R., Li, H., Tan, W., & Liu, D. (2020). In vitro antiviral activity and projection of optimized dosing design of hydroxychloroquine for the treatment of severe acute respiratory syndrome coronavirus 2 (SARS-CoV-2), 1–8. *Clinical Infectious Diseases*. . https://doi.org/10.1093/cid/ciaa237

Yuan, Y., Cao, D., Zhang, Y., Ma, J., Qi, J., Wang, Q., Lu, G., Wu, Y., Yan, J., Shi, Y., Zhang, X., & Gao, G. F. (2017). Cryo-EM structures of MERS-CoV and SARS-CoV spike glycoproteins reveal the dynamic receptor binding domains. *Nature Communications*, *8*, 15092–15099. https://doi.org/10.1038/ncomms15092

Yuldashev, M. P. (2002). Flavonoids of the aerial part of Trigonella grandiflora. *Chemistry of Natural Compounds*, *38*(3), 291–292. https://doi.org/10.1023/A:1020448531522

Zhang, X. Q., and Xu, L. S. (1989). Determination of avicularin in Polygonum aviculare L. by square wave polarography. *Proc Chin Acad Med Sci Peking Union Med Coll*, *4*(4),193–195.

Zhang, H., Penninger, J. M., Li, Y., Zhong, N., & Slutsky, A. S. (2020). Angiotensin-Converting Enzyme 2 (ACE2) as a SARS-CoV-2 receptor: Molecular mechanisms and potential therapeutic target. *Intensive Care Medicine*, *46*(4), 586–590. https://doi.org/10.1007/s00134-020-05985-9

Zhou, P., Yang, X.-L., Wang, X.-G., Hu, B., Zhang, L., Zhang, W., Si, H.-R., Zhu, Y., Li, B., Huang, C.-L., Chen, H.-D., Chen, J., Luo, Y., Guo, H., Jiang, R.-D., Liu, M.-Q., Chen, Y., Shen, X.-R., Wang, X., … Shi, Z.-L. (2020). A pneumonia outbreak associated with a new coronavirus of probable bat origin. *Nature*, *579*(7798), 270–273. https://doi.org/10.1038/s41586-020-2012-7

Zhou, Y., Hou, Y., Shen, J., Huang, Y., Martin, W., & Cheng, F. (2020). Network-based drug repurposing for novel coronavirus 2019-NCoV/SARS-CoV-2. *Cell Discovery*, *6*(1), 14 . https://doi.org/10.1038/s41421-020-0153-3